Supplemental information

RANK ligand converts the NCoR/HDAC3 co-repressor to a PGC1β- and RNA-dependent co-activator of osteoclast gene expression

Yohei Abe, Eric R. Kofman, Maria Almeida, Zhengyu Ouyang, Filipa Ponte, Jasmine R. Mueller, Grisel Cruz-Becerra, Mashito Sakai, Thomas A. Prohaska, Nathanael J. Spann, Ana Resende-Coelho, Jason S. Seidman, Joshua D. Stender, Havilah Taylor, Weiwei Fan, Verena M. Link, Isidoro Cobo, Johannes C. M. Schlachetzki, Takao Hamakubo, Kristen Jepsen, Juro Sakai, Michael Downes, Ronald M. Evans, Gene W. Yeo, James T. Kadonaga, Stavros C. Manolagas, Michael G. Rosenfeld and Christopher K. Glass

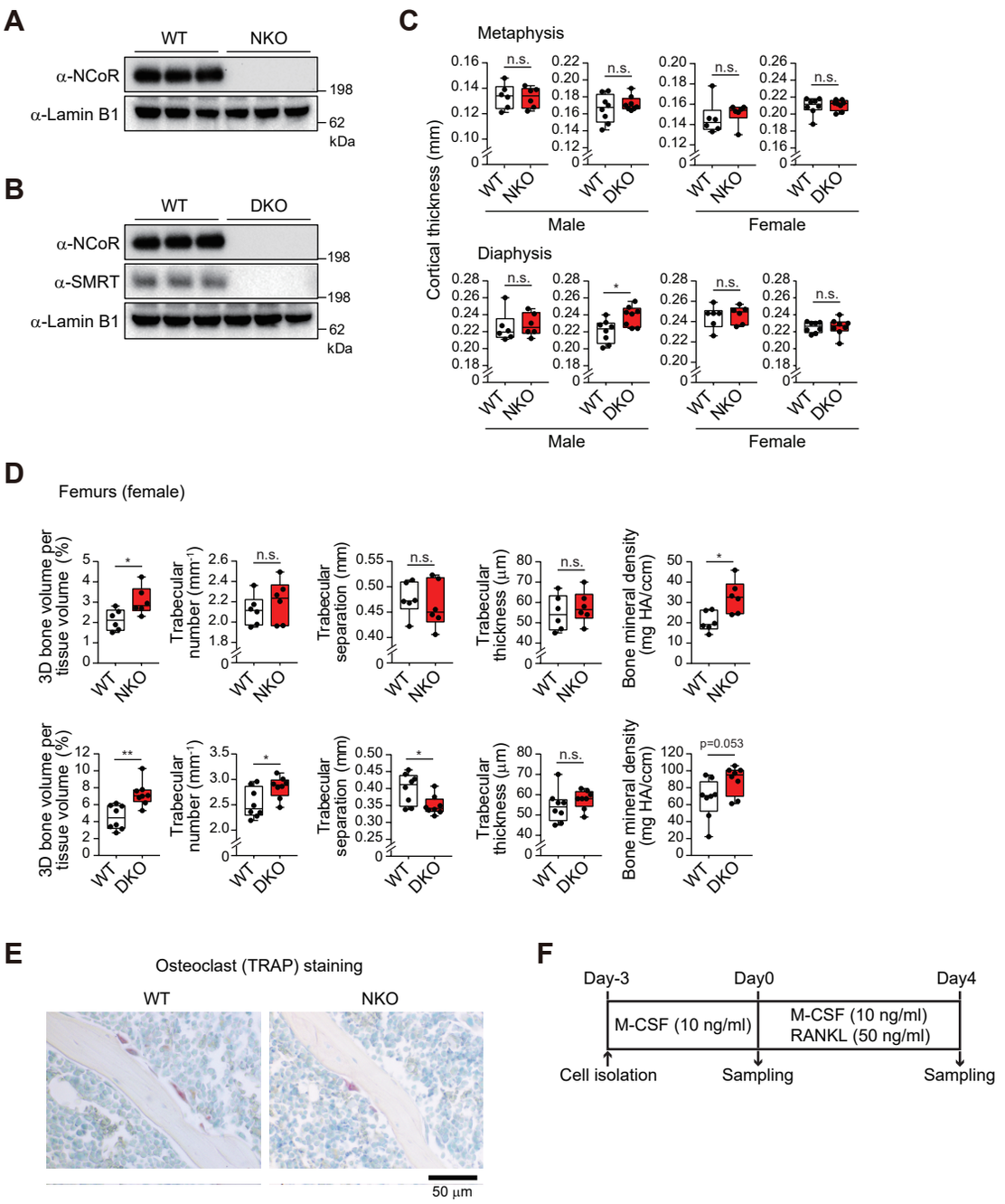

Figure S1. NCoR is required for osteoclast differentiation and normal bone development, Related to Figure 1

(A) Immunoblot analysis for NCoR protein in whole-cell lysates of bone marrow-derived macrophages from WT and NKO mice (12-week-old male, n=3 each).

(B) Immunoblot analysis for NCoR and SMRT proteins in whole-cell lysates of bone marrow-derived macrophages from WT and DKO mice (12-week-old male, n=3 each).

(C) Cortical thickness of metaphysis or diaphysis from 5-month-old male or female WT and NKO or DKO mice determined by μCT analysis. All box plots show the interquartile range. Data are mean ± s.d. (n=6-8 each). Student's t-test was performed for comparisons. *$p < 0.05$ was considered statistically significant.

(D) Trabecular bone volume, trabecular number, trabecular separation, trabecular thickness and bone mineral density in the femurs from 5-month-old female WT and NKO or DKO mice determined by μCT analysis. All box plots show the interquartile range. Data are mean ± s.d. (n=6-8 each). Student's t-test was performed for comparisons. *$p < 0.05$ and **$p < 0.01$ were considered statistically significant.

(E) Representative TRAP-stained cell images showing the effect of NKO on the femurs in 5-month-old male mice.

(F) Bone marrow cells were cultured in media with M-CSF for 3 days, and then treated with M-CSF plus RANKL for 4 days to differentiate to osteoclasts.

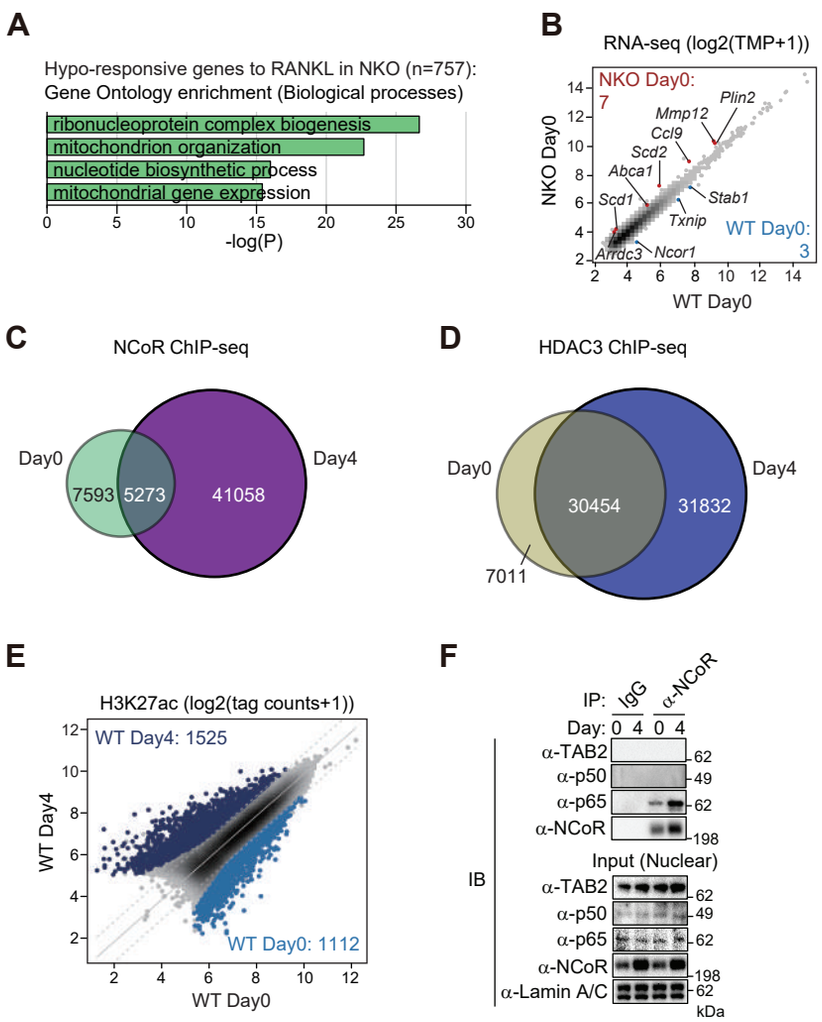

Figure S2. NCoR/HDAC3 complexes bind to RANKL-induced enhancers and promoters, Related to Figure 2

(A) The significant gene ontology terms associated with the hypo-responsive genes (Figure 2A) are shown.

(B) Scatter plot of RNA-seq data showing NKO-regulated gene expression in the absence of RANKL (light blue dots: significantly NKO-suppressed genes, light red dots: significantly NKO-induced genes, FDR < 0.05, FC > 1.5).

(C, D) The overlap between IDR-defined NCoR (C) or HDAC3 (D) ChIP-seq peaks at Day0 and at Day4 is shown by Venn diagram.

(E) Scatter plot of normalized H3K27ac ChIP-seq tags having at least 16 tags associated with ATAC-seq IDR peaks at Day0 in a 1000 bp window. RANKL-induced H3K27ac peaks (FDR < 0.05, FC > 2) are color-coded (light blue dots: significantly lost H3K27ac by RANKL treatment, dark blue dots: significantly gained H3K27ac by RANKL treatment).

(F) Immunoblot (IB) analysis showing interaction of NCoR with NFκB-p65 but not TAB2 or NFκB-p50 in bone marrow cells treated with or without RANKL for 4 days. Nuclear fraction was subjected to immunoprecipitation (IP) using anti-NCoR antibody followed by IB analysis with anti-TAB2, p50, p65 or NCoR antibody.

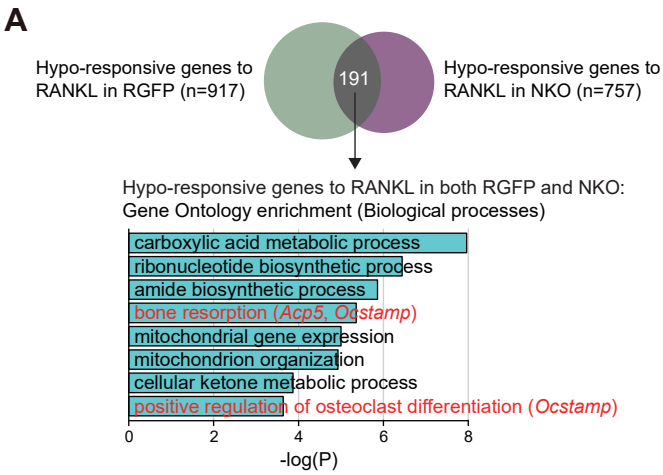

Figure S3. NCoR and HDAC3 activity are required for RANKL-induced H3K27 acetylation, Related to Figure 3
(A) The overlap between hypo-responsive genes in RGFP966-treated cells and NKO cells (Figure 2A) to RANKL. The significant gene ontology terms associated with the hypo-responsive genes to RANKL in both RGFP966 and NKO are shown.

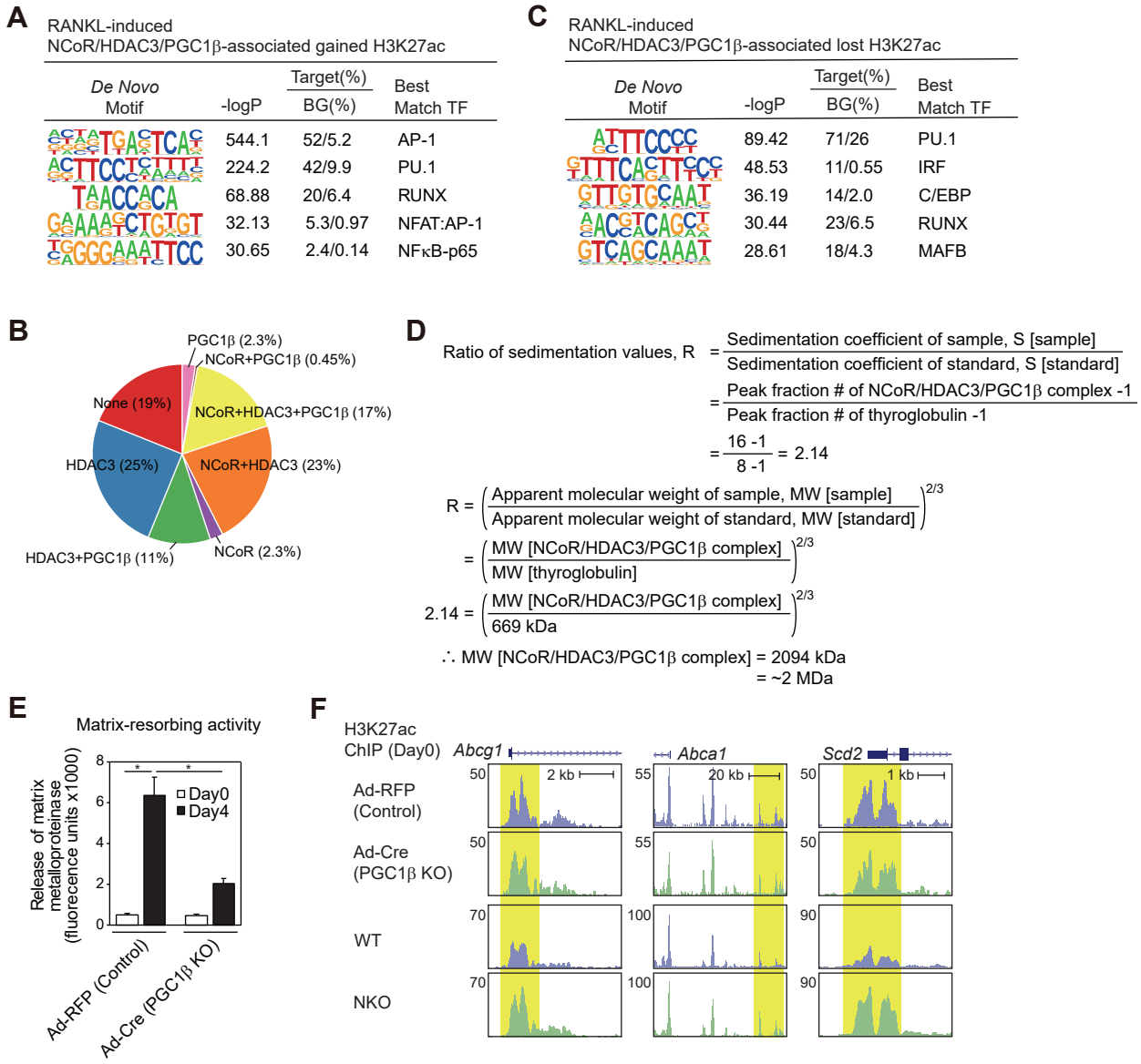

Figure S4. RANK signaling induces NCoR/HDAC3/PGC1β interaction required for H3K27 acetylation, Related to Figure 4

(A) *De novo* motif enrichment analysis of RANKL-induced NCoR/HDAC3/PGC1β-associated gained H3K27ac peaks (Figure 4C) using a GC-matched genomic background.

(B) The overlaps of ATAC-defined lost H3K27ac peaks in the presence of RANKL (n=1112 in Figure S2E) with NCoR, HDAC3 and/or PGC1β ChIP-seq peaks at Day4 are shown by pie chart.

(C) *De novo* motif enrichment analysis of RANKL-induced NCoR/HDAC3/PGC1β-associated lost H3K27ac peaks (Figure S4B) using a GC-matched genomic background.

(D) Assuming simillar partial specific volumes between thyroglobulin and NCoR/HDAC3/PGC1β complex, the molecular weight of the NCoR/HDAC3/PGC1β complex was estimated based on formulas described by Martin and Ames, 1961.

(E) RANKL-induced matrix-resorbing activity on *Pgc1b*$^{f/f}$ bone marrow cells expressing adenovirus-directed Cre recombinase. Data are mean ± s.e.m. (n=3 biological replicates). Analysis of variance was performed followed by Tukey's post hoc comparison. *p < 0.05 was considered statistically significant.

(F) Genome browser tracks of H3K27ac ChIP-seq peaks in the vicinity of the *Abcg1*, *Abca1* and *Scd2* loci at Day0. Yellow shading: NKO-induced peaks.

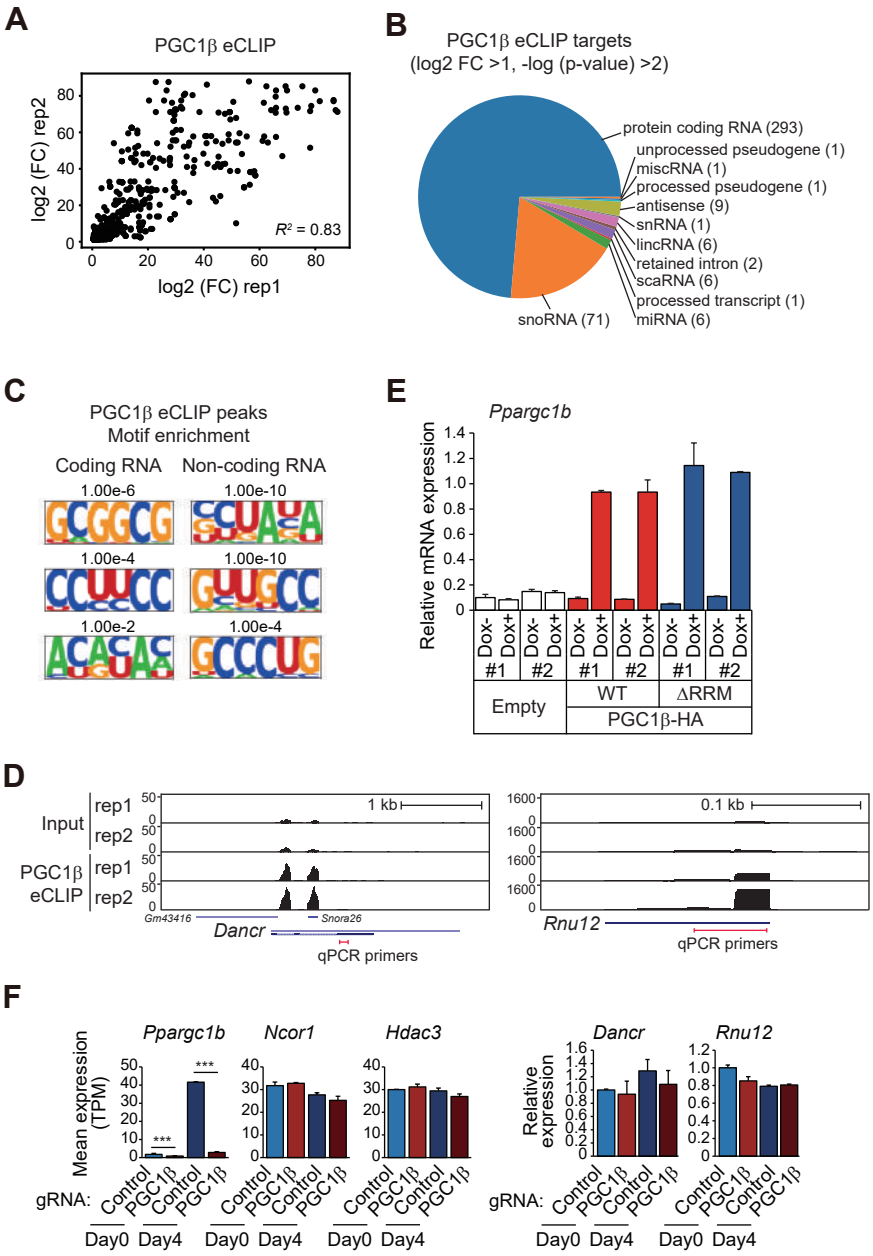

Figure S5. The PGC1β RRM mediates RNA-dependent interaction with NCoR/HDAC3 complexes, Related to Figure 6

(A) eCLIP with anti-PGC1β antibody in RAW 264.7 cells treated with RANKL for 4 days. Peaks were called on eCLIP replicates using matched inputs as controls, and overlapping high-confidence peaks (n=609, log2 fold change (FC) >1, -log (p-value) >2) exhibited a correlation coefficient of 0.83 in their log2 FC values.

(B) The target-level breakdown of PGC1β eCLIP peak binding sites.

(C) Motif analysis of PGC1β eCLIP peaks split between protein-coding and non-coding RNAs.

(D) Genome browser tracks showing PGC1β eCLIP peaks on non-coding RNA *Dancr* (left) and *Rnu12* (right).

(E) PGC1β transcript (*Ppargc1b*) expression in HA-tagged PGC1β (WT or ΔRRM) or the empty (Emp) vector-introduced RAW 264.7 cells in the presence or absence of doxycycline (Dox). Data are mean ± s.d. (n=2 biological replicates).

(F) Bar plots for expression of *Ppargc1b*, *Ncor1*, *Hdac3*, *Dancr* and *Rnu12* in PGC1β or control gRNA-introduced Hoxb8 cells at Day0 and Day4 after RANKL treatment. The significance symbols indicate statistical significance, ***p-adj < 0.001 reported by DESeq2 using the Benjamini-Hochberg method for the multiple-testing correction.

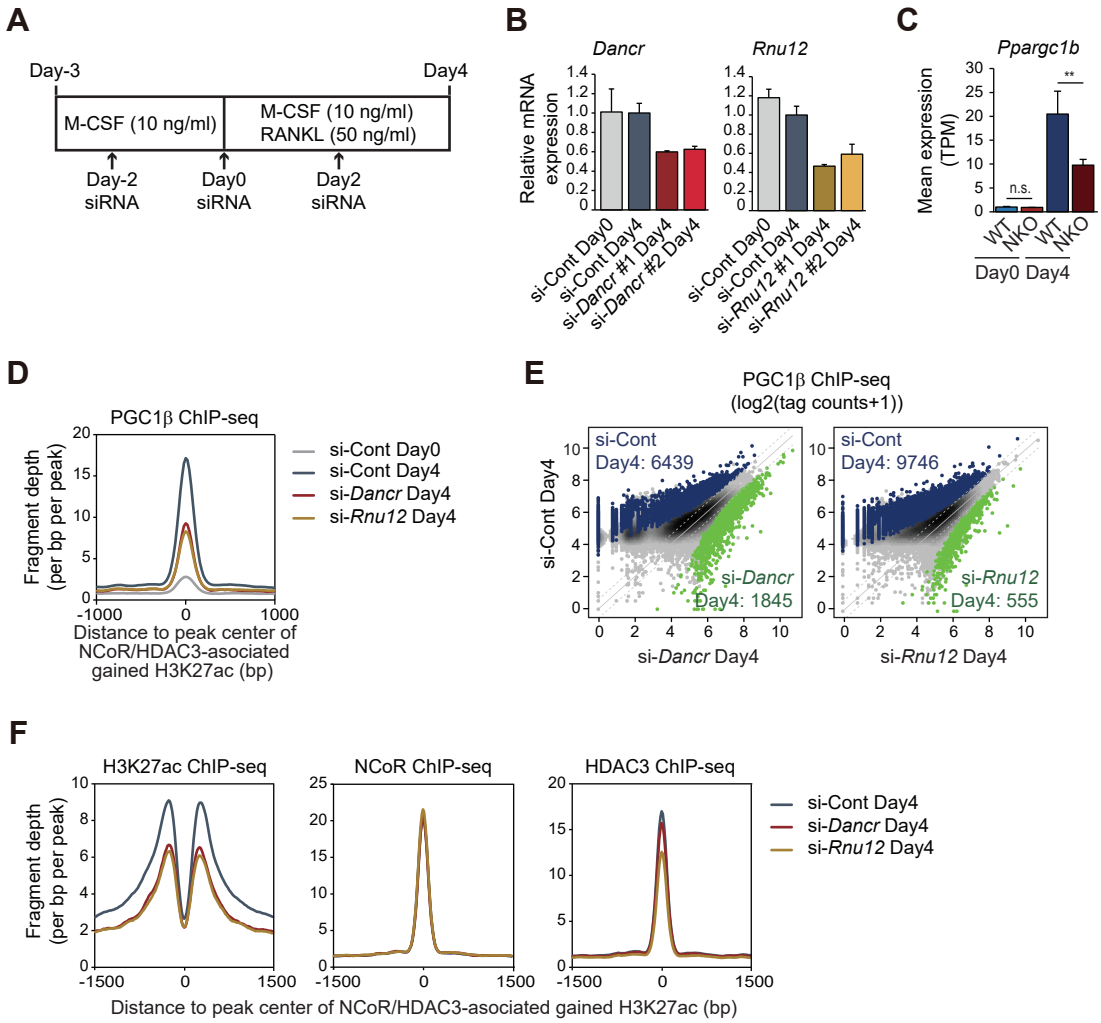

Figure S6. *Dancr* and *Rnu12* are required for RANKL-induced osteoclast differentiation, Related to Figure 7

(A) Bone marrow cells were cultured in media with M-CSF for 3 days, and then treated with M-CSF plus RANKL for 4 days to differentiate to osteoclasts. siRNAs were transfected at Day -2, 0 and 2 with replacement of fresh media.

(B) Gene expression levels of *Dancr* and *Rnu12* in bone marrow cells transfected with si-Cont, si-*Dancr* (#1, #2) or si-*Rnu12* (#1, #2) at Day0 and Day4 after RANKL treatment. Data are mean ± s.d. (n=2 biological replicates).

(C) Bar plot for expression of *Ppargc1b* in bone marrow cells from WT or NKO mice at Day0 and Day4 after RANKL treatment. The significance symbols indicate statistical significance, **p-adj < 0.01 reported by DESeq2 using the Benjamini-Hochberg method for the multiple-testing correction.

(D) Normalized distribution of PGC1β ChIP-seq tag density in siRNA (si-Cont, si-*Dancr* or si-*Rnu12*)-introduced bone marrow cells at the vicinity of NCoR/HDAC3-associated gained H3K27ac peaks in WT at Day4 after RANKL treatment (n=2757 in Figure 2C).

(E) Scatter plot of normalized PGC1β ChIP-seq tags in si-Cont at Day4 vs. si-*Dancr* (left panel) or si-*Rnu12* (right panel) at Day4. PGC1β peaks regulated by *Dancr* or *Rnu12* knockdown (FDR < 0.05, FC > 1.5) are color-coded (dark blue dots: significantly lost PGC1β peaks, green dots: significantly gained PGC1β peaks).

(F) Normalized distribution of H3K27ac, NCoR or HDAC3 ChIP-seq tag density in siRNA (si-Cont, si-*Dancr* or si-*Rnu12*)-introduced bone marrow cells treated with RANKL for 4 days at the vicinity of NCoR/HDAC3-associated gained H3K27ac peaks in WT at Day4 after RANKL treatment (n=2757 in Figure 2C).

Antibody		Source	Catlog No / Clone No	Dilutions / Concentrations
anti-NCoR	Monoclonal	Dr. Hamakubo	IgG-Y8129	5 μg/assay for ChIP
				2 μg/assay for IP
				1 μg/ml for IB
				1 μg/assay for RIP
anti-SMRT	Polyclonal	Novus	NB100-58826	0.2 μg/ml for IB
anti-HDAC3	Polyclonal	GeneTex	GTX113303	3 μg/assay for ChIP
				2 μg/assay for IP
				0.32 μg/ml for IB
				1 μg/assay for RIP
anti-PU.1	Polyclonal	Santa Cruz	sc-352 / T-21	2 μg/assay for ChIP
anti-p65	Polyclonal	Santa Cruz	sc-372 / C-20	2 μg/assay for ChIP
				2 μg/ml for IB
anti-p50	Polyclonal	Santa Cruz	sc-1190 / C-19	1 μg/ml for IB
anti-Fosl2	Monoclonal	Santa Cruz	sc-166102 / G-5	4 μg/assay for ChIP
anti-PGC1β	Monoclonal	Abcam	ab176328	1 μg/assay for ChIP
				1 μg/assay for IP
				0.1 μg/ml for IB
				1 μg/assay for RIP
				1 μg/assay for eCLIP
anti-Acetylated-Lysine	Monoclonal	Cell signaling Technology	#9441	1:1000 for IB
anti-H3K27ac	Polyclonal	Active Motif	#39133	2 μg/assay for ChIP
anti-ACP5	Monoclonal	Millipore	MABF96 / 9C5	0.5 μg/ml for IB
anti-TAB2	Polyclonal	Proteintech	14410-1-AP	1:1000 for IB
anti-TBL1	Monoclonal	Santa Cruz	sc-137006 / H-3	1 μg/ml for IB
anti-FLAG	Monoclonal	Sigma-Aldrich	F1804	0.2 μg/ml for IB
				0.5 μg/assay for IP
anti-HA tag	Polyclonal	Abcam	ab9110	1 μg/assay for RIP
anti-Lamin B1	Monoclonal	Santa Cruz	sc-374015 / B-10	0.1 μg/ml for IB
anti-Lamin A/C	Polyclonal	Cell signaling Technology	#2032	1:1000 for IB
anti-β-Actin	Monoclonal	Sigma-Aldrich	A2228 / AC-74	1:5000 for IB

Table S1. Detailed information about antibodies, Related to STAR Methods